Journal of Photonic Materials and Technology
2021; 7(1): 8-15
http://www.sciencepublishinggroup.com/j/jpmt
doi: 10.11648/j.jmpt.20210701.12
ISSN: 2469-8423 (Print); ISSN: 2469-8431 (Online)

High Optical Reflection in Two-dimensional ZnO-Si Photonic Crystals Induced by Coupled Optical Micro-cavities

José Antonio Medina-Vázquez, Evelyn Yamel González-Ramírez, José Guadalupe Murillo-Ramírez*

Department of Materials Physics, Advanced Materials Research Center (CIMAV), Chihuahua Chih., Mexico

Email address:

jose.medina@cimav.edu.mx (J. A. Medina-Vázquez), evelyn.gonzalez@cimav.edu.mx (E. Y. González-Ramírez), jose.murillo@cimav.edu.mx (J. G. Murillo-Ramírez)

*Corresponding author

To cite this article:

José Antonio Medina-Vázquez, Evelyn Yamel González-Ramírez, José Guadalupe Murillo-Ramírez. High Optical Reflection in Two-dimensional ZnO-Si Photonic Crystals Induced by Coupled Optical Micro-cavities. *Journal of Photonic Materials and Technology*. Vol. 7, No. 1, 2021, pp. 8-15. doi: 10.11648/j.jmpt.20210701.12

Received: June 21, 2021; **Accepted**: July 5, 2021; **Published**: July 9, 2021

Abstract: Photonic crystals can exhibit relevant optical properties when transmitting or reflecting a light beam. In particular in a two-dimensional photonic crystal the reflective properties can be of interest and consequently optimized for different technological applications such as tunable laser cavities, photovoltaic solar systems, and selective high reflection mirrors among many others. Taking this motivation into account, a study of the reflective optical properties of two-dimensional photonic crystals built on a hybrid substrate of ZnO:Si has been developed. The aim of the present research is to demonstrate the feasibility to control the optical reflectance spectra of a two-dimensional photonic crystal by the inclusion of an array of optical micro-cavities in a regular photonic structure. Moreover, in this research an explanation of the origin of the high optical reflectance predicted by numerical calculations and confirmed by experimental measurements in a photonic crystal that contains an array of micro-optical cavities is also given. The results of numerical calculations of the optical properties of one of the photonic crystals studied determined that the origin of the increase in its optical reflectance is the light emission from the silicon present in the ZnO-Si substrate where the photonic structure was built. Strong resonant modes of the optical electric field stablished mainly in silicon present in two types of resonant cavities recognized in the photonic crystal favor the stimulated emission of light that gives rise to the high optical reflectivity.

Keywords: Photonic Crystals, Optical Cavity, Stimulated Emission, Purcell Factor

1. Introduction

Photonic crystals are one of the most novels and promising developments in the materials research area, their ability to control the flow of photons in matter confers them this importance. A photonic structure is capable of acting as a selective transmitter/absorber of light, a beam splitter, a wave guide, a light extractor in light emission diodes (LEDs) and, in general, a light processor in optical integrated circuits [1-5]. Certainly, these and other novel applications of photonic crystals can potentially be used to replace or improve specific functions currently developed by electronic devices, and of course with some significant advantages such as the processing speed comparable to the speed of light in vacuum. Photonic devices can be used in various interest areas such as telecommunications, for example, in the modulation and wavelength division multiplexing at low energetic cost, among many others potential uses [5-9].

Two-dimensional photonic crystals are of great interest because they are relatively simple to manufacture using techniques developed for the electronics industry, such as chemical assisted ion beam etching (CAIBE), reactive ion etching (RIE) and also using more modern techniques such as the focused ion beam milling (FIB) among others [10, 11].

The goal of the present research is to demonstrate the feasibility to control the optical reflectance spectra of a two-dimensional photonic crystal by the inclusion of an array of optical micro-cavities in the photonic structure. As well as

explaining the origin of the high optical reflectance in a two-dimensional photonic crystal that contains an array of micro-optical cavities. In other words, it is proposed in this work the use of optical micro-cavity arrays in order to obtain a strong wave coupling in a photonic structure that can enhance its reflective properties at a desired wavelength.

The effects of introducing an optical cavity or a pair of them into a photonic crystal have already been studied in research reports published in the literature [12]. These cavities or defects considered usually are described either by a point defect or also by a linear section of these defects, creating a waveguide [13-15]. Highly nonlinear wave resonance effects exhibited by oscillation modes established in the cavity have been found [16]. Moreover, wave coupling effects have also been found as a result of the interaction between the established oscillation modes and the structural defects that break the periodicity of holes defining the photonic crystal, usually in a triangular lattice [17, 18].

In the present work we have considered a two-dimensional photonic crystal with a square lattice including an embedded square array of quasi-circular micro-cavities whose sizes are around one order of magnitude larger than the diameter of the circular cylindrical air holes describing the ordinary photonic crystal. This configuration considered for a photonic crystal studied in the present work has been found to have the ability to significantly increase the reflectance at a specific wavelength determined by its structural parameters. Thus, by varying the structural parameters of the fabricated photonic crystal, including both, its diameter and the lattice parameter of the micro-cavities array, it is possible to obtain a device with a tunable high reflectance at a specific wavelength. The relevance of these findings is precisely the contribution of this work which can be of help in the optimization of tunable laser cavities, between other novel developments.

2. Methods and Experimental Details

2.1. Numerical Simulations

At the first step of this research numerical simulations of the optical properties of two PhCs using both, software developed by our research group based on the finite element technique and commercial software such as Comsol Multiphysics were performed [19]. In calculations developed were assumed a set of structural parameters defining two types of photonic structures; one of the photonic crystals which was taken as the control sample (PhC1) describes a periodic regular structure of square lattice with a lattice constant $a_{contrl.}$=1.0 μm and circular cylindrical holes filled with air having a radius of $r_{contrl.}$=0.25 μm and a depth equal to 1 μm. A hybrid substrate composed by a ZnO thin film with a thickness of 230 nm deposited on a silicon plate was assumed. The other photonic crystal (PhC2) called the test sample, is also assumed to be built on the same substrate as the control sample. In addition, the PhC2 includes a quasi-circular cavity pattern with a diameter of 10 μm, describing a second square lattice. This array of quasi-circular cavities with a different lattice constant in the test PhC2 was embedded in a regular square lattice of cylindrical air holes similar to that defines the control sample PhC1. The optical cavities array in the test sample PhC2 describes regions in which there are no air holes. The array of quasi-circular micro-cavities had a diameter of d_c=10 μm and an approximated lattice constant of a_c=30 μm as shown in Figure 1 (a) and (b). The dependence of the refractive index on the wavelength for both, the ZnO thin film and the silicon substrate was taken into account in calculations. The optical properties obtained from the numerical calculations included the photonic band structure and the spectral optical reflectance of each photonic crystal considered in this research. The stimulated emissions of light in silicon and the spatial distribution of the optical electric field describing the resonant modes established in the optical cavities array incorporated in the PhC2 sample were also obtained.

2.2. Sample Preparation

Two slab samples of two-dimensional photonic crystals similar to those assumed in numerical calculations were fabricated on a silicon plate substrate [001] coated with a ZnO thin film of approximately 240 nm thicknesses deposited by Assisted Chemical Vapor Deposition (AACVD) method. One of the photonic structures, the test PhC2 sample, was built on a ZnO-Si substrate in an area of 84×84 μm^2 while the other sample called control sample PhC1, was built in an area of 30 ×30 μm^2 using a JEOL JEM 9320-FIB Focused Ion Beam (FIB) system with Ga+ ion source operated at 26.5 kV. Both photonic crystals, the PhC1 and PhC2, were built using the same structural parameters assumed in numerical calculations. These structural parameters of the control sample PhC1 and the test sample PhC2 were achieved by setting a dose of 200 $nC/\mu m^2$ and 1000 pA of irradiated current during 15 seconds per hole using the spot milling shape [20]. Figures 2 (a) and (b) show SEM micrographs of the PhC1 and PhC2 built samples, respectively.

2.3. Optical Characterization of Photonic Structures

Each one of the PhCs built was optically characterized by measuring its spectral optical reflectance at normal incidence using an experimental setup described elsewhere [20]. The optical characterization of the PhCs was performed using eight single mode laser diodes available in our lab with stabilized output power, coupled to an optical fiber having wavelengths equals to 633 nm, 750 nm, 785 nm, 852 nm, 1308 nm, 1392 nm, 1547 nm and 1594 nm, respectively. Each of light beams used was linearly polarized to ensure only the measurement of light reflected by the PhCs avoiding to detect any non-desired optical signals.

3. Results and Discussion

3.1. Numerical Simulations

From numerical calculations developed in this research, several remarkable findings about the optical properties of each PhC considered were obtained. First, it was found an

unusual behavior of the spectral optical reflectance of the photonic crystal containing the optical cavities array. Figure 1 (c) shows the optical reflectance calculated for the two photonic crystals studied in this research, the measurement for the control sample PhC1 is denoted by a dashed line and for the other sample including an array of optical cavities, the sample PhC2, is denoted by a continuous solid black line. As can be observed in Figure 1 (c), the optical reflectance calculated for the PhC2 shows a significant increase in the wavelength range from 700 to 800 nm, regarding to the value obtained for the PhC1 sample at the same wavelength range. Specifically, the optical reflectance of the PhC2 sample, containing the cavities array, slightly exceeds the 80% at a wavelength centered at 750 nm while for the PhC1 sample at this wavelength barely was obtained 10%. Although, it was also obtained a slightly enhancement of the optical reflectance in the wavelength ranges from 850 to 1050 nm for the PhC2, regarding the values obtained for the PhC1. Clearly, the optical cavities array present in the PhC2 sample plays a relevant role in the extraordinary increase of its optical reflectance in the wavelength range from 700 to 800 nm, which will be discussed in the next sections.

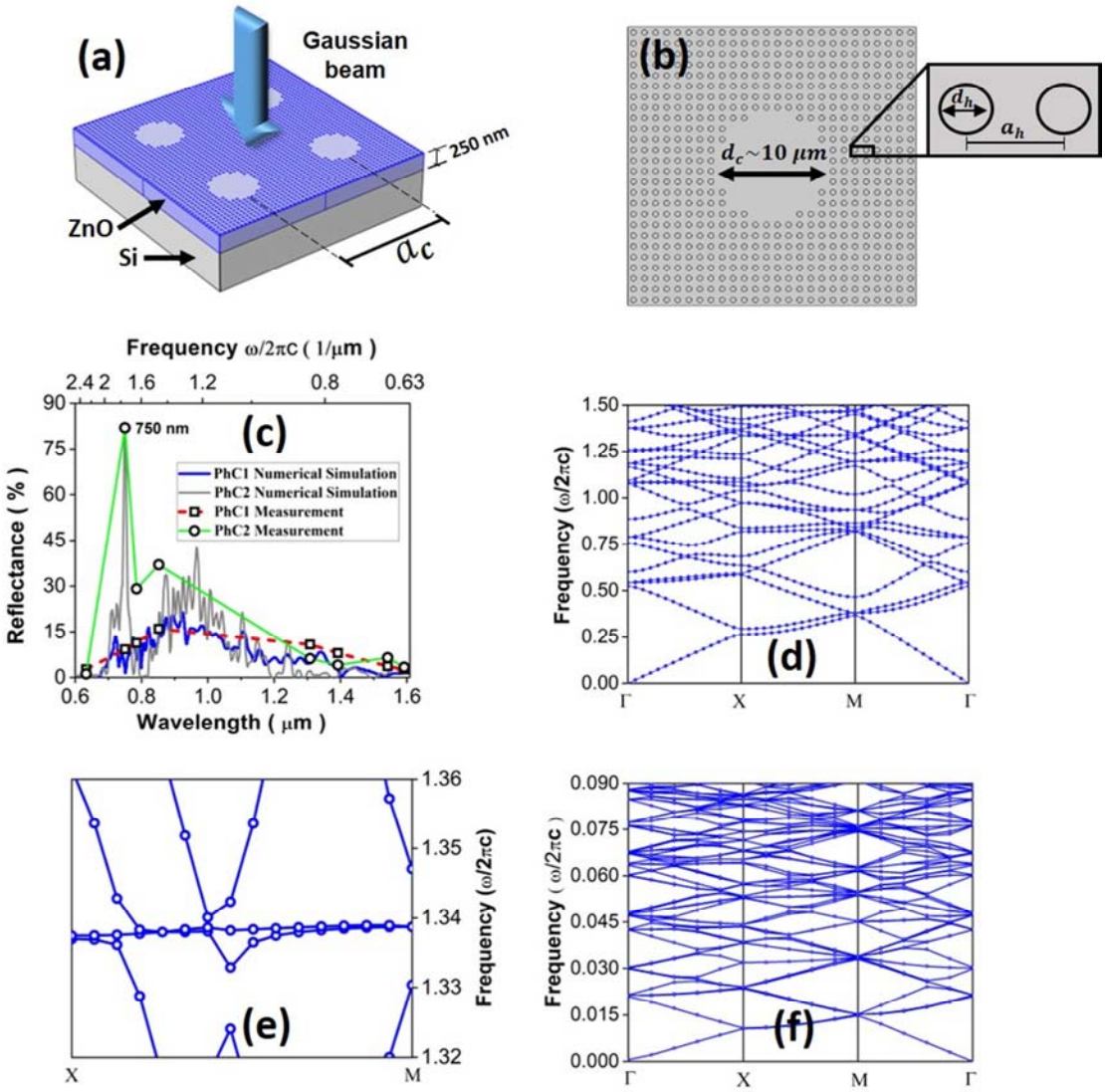

Figure 1. *(a) Schematic diagram of the structural parameters of a section of the photonic crystal PhC2 considered in numerical simulations, (b) a section of the PhC2 showing the holes diameter* d_h*, and the lattice constant* a_h *of the square array of air-filled holes, and the diameter* d_c *of one of the optical cavities. (c) Calculated optical reflectance for the control sample PhC1 represented by a dashed line, and the test sample PhC2 denoted by a continuous solid black line, respectively. The squares and the dots represent the experimental measurements for the PhC1 and PhC2, respectively, which have been joined by a dashed blue line and a solid green line, respectively, for eye guidance only. (d) Numerical calculation of the photonic band structure for the control sample PhC1 composed only by a regular square lattice of air-filled holes milled in a ZnO-Si two-layer substrate, (e) an amplification of the photonic band structure of the PhC1 sample, in the frequency range from 1.32 to 1.36 ω/2πc (corresponding to the wavelength range of incident light from 700 to 800 nm), (f) a part of the photonic band structure calculated for the PhC2 sample including a square array of optical cavities, corresponding to the frequency range from 0.0 to 0.09 in units of ω/2πc.*

3.2. Photonic Band Calculation

Numerical simulations performed included the calculations of the photonic bands structure of both samples studied. Periodic boundary conditions (PBC) to take into account the periodicity of the structural parameters that defines each PhC studied were assumed. Figures 1 (d) and (f) show the photonic

bands structure of the two photonic crystals studied in this work. Figure 1 (d) shows the photonic band structure of the control sample PhC1 composed only by a regular square lattice of air holes, while figure 1 (f) shows the photonic band structure of the PhC2 sample that includes a regular square lattice of air holes as the PhC1 and additionally a square array of optical cavities. In fact, in figure 1 (f) we only show a part of the photonic band structure calculated for the PhC2 sample corresponding to the frequency range from 0.0 to 0.09 in units of $\omega/2\pi c$ (representing c the light speed in vacuum and ω the angular frequency of radiation) even when calculations were performed beyond $0.09\omega/2\pi c$ value. The above due to it was obtained that there is a large quantity of photonic bands for the PhC2 sample, which constitute practically a continuous succession of allowed propagation frequencies above the frequency $0.09\ \omega/2\pi c$. It is remarkable to observe in figure 1 (d) that the photonic band structure calculated for the PhC1 sample does not present any complete photonic band gap around the normalized frequency corresponding to the wavelength range where the optical reflectance had an enhancement. This fact can be easily confirmed in figure 1 (e) where an amplification of the photonic band structure, obtained for the PhC1 sample, in the frequency range from 1.32 to 1.36 $\omega/2\pi c$ (corresponding to the wavelength range of incident light from 700 to 800 nm) shows a continuous allowed band. Therefore, it is plausible to understand that the high optical reflectance in the PhC2 sample it is not associated either with the existence of a complete photonic band gap. One can come to this conclusion due to there is a great similarity between the photonic band structure calculated for both, the control sample PhC1 and the PhC2 sample as shown in Figures 1 (d) and (f). The only appreciable difference between both photonic band structures shown in figures 1 (d) and (f) is the existence of a large quantity of bands associated to the sample PhC2 for the corresponding frequency ranges in both photonic bands structures. In fact, it is reasonable to expect that the photonic bands structure of PhC2 be essentially the same photonic bands structure obtained for the PhC1 sample. Except that the cavities array present in PhC2 necessarily introduces a great quantity of allowed states in the frequency domain. This due to the optical cavities in the PhC2 sample are a continuous thin film region where no any air holes were milled what determines a large number of allowed bands below the frequency interval ranging from 1.32 to 1.36 $\omega/2\pi c$ in the photonic band structure.

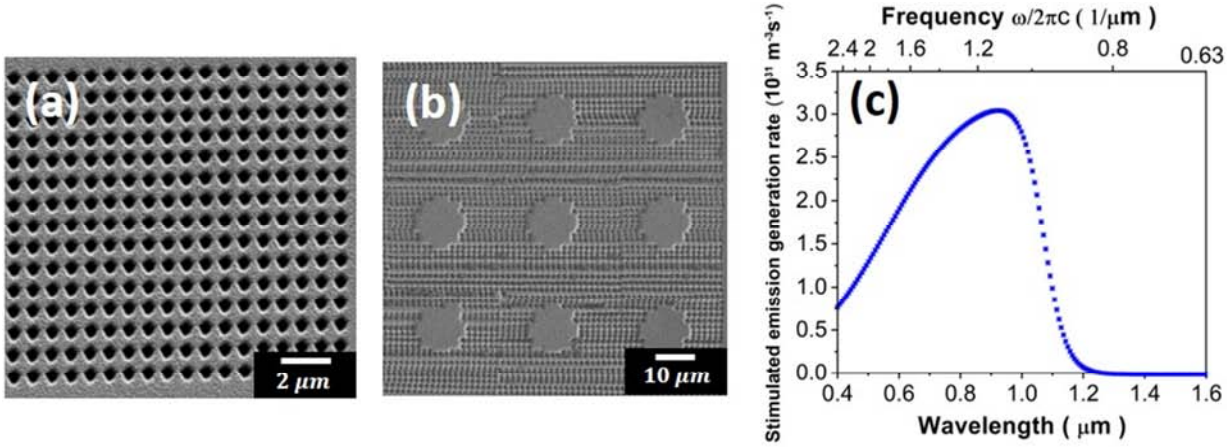

Figure 2. *(a) and (b) scanning electron microscope (SEM) micrographs of the PhC1 and the PhC2 samples, respectively. (c) Calculation of the stimulated emission generation rate in units of $1/(m^3s)$ as a function of the wavelength of incident radiation in silicon.*

3.3. Measurements of Optical Reflectance of Photonic Structures

After to obtain the extraordinary results from numerical calculations that predicts an increasing of the optical reflectance at specific wavelength ranges in the PhC2 sample regarding to the obtained results in the PhC1 sample, these two photonic crystals as described in section 2.2 were built. Figures 2 (a) and 2 (b) show scanning electron micrographs of the PhC1 and the PhC2 samples, respectively. Then, both samples PhC1 and PhC2 were optically characterized by measuring their optical reflectance at normal incidence. Figure 1 (c) shows the experimental measurements of the optical reflectance in the Vis-NIR range of the electromagnetic spectrum of the PhC1 and the PhC2, the control and test samples, respectively. As it can be observed in Figures 1 (c), the results from numerical calculations are in good agreement with the experimental measurements, except for the intervals where there are no measurements due to the fact that we do not have light sources in that range.

The finding predicted by numerical simulations was confirmed; clearly, the optical reflectance of PhC2 was enhanced respect to the obtained measurements for the PhC1 as shown in Figure 1 (c). The peak amplitude of the optical reflectance of PhC2 reached a value above 80% while the sample PhC1 barely reached a value around 15% as shown in Figure 1 (c). Due to this fact, this research was focused on finding the origin of the enhancement of the optical reflectance of the PhC2 sample at certain wavelength range. It was explained in Section 3.2 that the high optical reflectance in the PhC2 sample it is not associated with the existence of a complete photonic band gap, and therefore it is necessary to address another possible explanation.

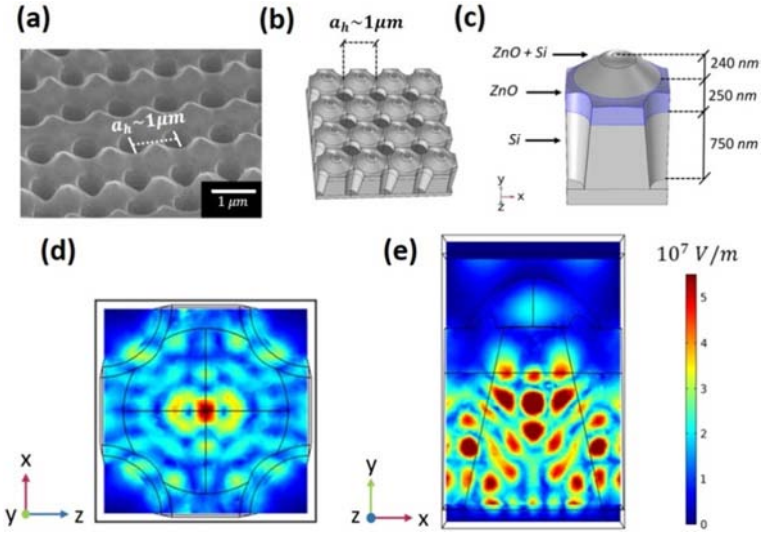

Figure 3. *(a) SEM micrograph taken at high amplification (20,000×) of a surface section of the PhC2 showing a mounds array (assumed as a mix of silicon and ZnO deposited over the ZnO thin film) surrounding the air holes as a result of a redepositing effect during the fabrication process with the FIB system. (b) Design of a photonic structure similar to that shown in (a) including a holes array surrounded by a set of structures composed by Si:ZnO mounds over a ZnO-Si two-layer, used in numerical simulations of optical properties of the PhCs studied. (c) Details of one of the structures that constitute the array shown in (b) identified as a type 1 resonant cavity. (d) (top view) and (e) (side view) of a typical two-dimensional spatial distribution of the optical electric field amplitude numerically calculated that is established in the PhC2 built on a ZnO-Si two-layer substrate containing a set of type 1 resonant optical cavities such as those shown in (b). The incident light beam had a wavelength of λ=750 nm, and the Purcell factor associated to the resonant cavities in the photonic structures was equal to 8.*

3.4. Stimulated Emissions in Silicon Connected with High Optical Reflectivity

In view of fact that the enhancement of the optical reflectance in the PhC2 sample in the wavelength range of 750 -1050 doesn't have a relation with a complete photonic bandgap as was discussed in section 3.2, we searched for its origin in the Si:ZnO substrate where the PhCs were built. First, the photon associated to the incident radiation with a wavelength of 750 nm does not have the energy required to promote a charge carrier from the valence band to the conduction band in the ZnO thin film. This because the band gap energy of ZnO thin film synthetized is 3.18 eV (measured value by our work team) and the energy of the photon associated to the wavelength of 750 nm is only 1.65 eV. Of course, it is required to promote the electrons to a high energy level so that they can eventually decay to a lower energy level generating a photon emitted. However, the excitation of electrons from the valence band to the conduction band using the energy of the photon associated to the radiation with a wavelength of 750 nm in silicon it is possible since its bandgap energy is equal to 1.2 eV. Therefore, it is reasonable to believe that the origin of the localized high optical reflectance in the PhC2 can be related to the presence of the silicon substrate as will be discussed below.

Recently, it has been reported that in silicon the electrons could gain enough energy and momentum to be promoted to high energy states in the first and second conduction energy band at about 1.8 eV and then have a transition to yield emissions around 750 nm [21]. Although, also other types of electron transitions can occur in silicon giving rise to emissions centered at 450 nm, 650 nm and 850 nm which has been measured in electronic assembled devices, specifically in Silicon Avalanche Mode Leds [21]. Nevertheless, the relevant fact about the origin of spectral characteristics of the 750-850 nm emission is that these are correlated to the scattering and diffusion of charge carriers which can be excited and confined in specific zones inside a device, allowing the enhance of predominant radiation in a specific wavelength range. In other words, it has been confirmed the correlation between the characteristics of the 750-850 nm emission and the existence of transitions of electrons between the first and the second conduction bands in silicon [21, 22]. Therefore, in the photonic crystals built on a substrate composed by a ZnO thin film deposited onto a silicon substrate studied in this research it is possible to induce and promote direct transitions of electrons from the valence band to the first or second conduction band. These electrons then can have relaxation transitions from the second to the first conduction band or transitions from the second conduction band to the valence band given rise to the emissions in 750 nm as has been confirmed in Refs. [21, 22]. Consequently, in our PhCs, the excitation of electrons in silicon is caused by the incident light that is highly transmitted by the thin film of ZnO which acts as an anti-reflective coating over the entire PhC2 area.

Moreover, as it will discussed now, the high optical reflection at certain wavelengths in the PhC2, is the result of the stimulated light emission in silicon connected with the strong optical electric fields that are established in specific regions of it. Figure 2 (c) shows a calculation of the stimulated emission generation rate in units of $1/(m^3 s)$ as a function of the wavelength of incident radiation in silicon. The stimulated emission generation rate W_{st} between an initial state $|i\rangle$ and a final state $|f\rangle$ is obtained directly from the golden rule of Fermi [23]:

$$W_{st} = \frac{2\pi}{\hbar}\langle f|H'|i\rangle^2 \delta\left(E_f - E_i - \hbar\omega\right) \quad (1)$$

where H' is the time-dependent electromagnetic perturbation, δ is the Dirac delta function, ω is the angular frequency of the emitted photon and E_i, E_f are the initial and final energies of the system, respectively.

It is important to recognize that in Figure 2 (c) appears every one of the possible emissions feasible to be stimulated in silicon. Therefore, is reasonable to assume that the high amplification of optical reflection in the PhCs measured and calculated in this work as shown in Figure 1 (c) can be determined by the presence of silicon substrate. Moreover, it is relevant to notice that the spectral characteristics of the 700-900 nm emission are located in the range of maximum stimulated emission generation rate in silicon.

Numerical calculations of the optical properties of the PhC considered in this research have also shown that the array of circular optical micro-cavities contained in the PhC2 together with the regions located around the array of air-filled holes that describe the ordinary PhC, act as a set of resonant cavities and both, contributes to the stimulated emission of light from the PhC2, leading to an enhancement of its optical reflectance [24]. The regions located around the array of holes filled with air that describes the ordinary PhC, constitute a particular cavity type (which will be called resonant type I cavity). These regions allow the establishment of strong and non-uniform optical electric fields. Figure 3 (a) shows a SEM micrograph of a section of the surface of the PhC2 that describes a set of type I resonant cavities in the ZnO:Si substrate, distributed periodically around the array of air holes. The mounds array surrounding the air holes in the PhC2 shown in Figure 3 (a) is the result of a redeposition effect during the fabrication process of the photonic structure by the FIB system, and thus, it can be assumed as a mixture of silicon and ZnO deposited over the ZnO thin film. Next, a representative type I cavity in PhC2, shown in Figures 3 (b) and 3 (c), was modeled and its optical properties were numerically simulated. The results obtained are shown in Figures 3 (d) and (e) which illustrates two-dimensional views of a typical spatial distribution of the optical electric field amplitude established in a type I optical cavity. This type of cavity is partially responsible for the stimulated emission of light that explains the high optical reflection at certain wavelengths in the PhC2. The amplitude of the optical electric field shown in Figures 3 (d) and (e) is described by colors ranging from blue (low) to red (high). As can be observed in Figures 3 (d) and (e) the optical electric field established in a representative type 1 cavity has a sophisticated spatial distribution with intensities as high as 7×10^7 V/m. These electric field intensities are clearly sufficient to promote electrons from the valence band to high energy levels in the conduction band in silicon and then have a transition to yield stimulated light emission.

As is well known, the Purcell factor is a parameter that characterizes the enhancement of spontaneous and stimulated emission rate of a resonant cavity as a result of electron-photon interactions [25-27] and it is given by the following relation:

$$F_P = \frac{3Q\left(\frac{\lambda}{n}\right)^3}{4\pi^2 V_{eff}} \quad (2)$$

where Q is the quality factor of the cavity, λ is the resonant free space wavelength of the cavity, n is the refractive index at the location where the square electric field is maximum ($|E(r_{max})|^2$), and V_{eff} is the effective volume occupied by the electromagnetic energy of the resonant mode. V_{eff} is defined as the ratio of the total electric field energy to the peak value of the electric field energy density [27, 28]:

$$V_{eff} = \frac{\int \varepsilon(r)|E(r)|^2 d^3r}{\varepsilon(r_{max})|E(r_{max})|^2} \quad (3)$$

where ε (r) is the dielectric constant in the material and E(r) is the electric-field amplitude at the position r.

From numerical calculations of the optical properties of the photonic structure comprising the set of ZnO:Si mounds deposited over a structure ZnO-Si shown in Figure 3 (a), it was found that for one of these resonant cavities as shown in Figure 3 (b), the quality factor had a value Q=58.911. In contrast, the effective volume occupied by the electromagnetic energy of the resonant mode had a very low value equal to V_{eff}=4.3634× 10^{-21} m^3=1.8509 $(\lambda/n)^3$. Both, the quality factor Q and the V_{eff} determined a Purcell factor larger than the unity which explains the enhancement of the spontaneous and stimulated emission of the resonant cavity [29]. Moreover, Figures 3 (d) and (e) clearly show that the intensity of the optical electric field amplitude established in a representative resonant type 1 cavity has maximum values in the volume corresponding to Si plate. Although, it reaches a little penetration into the ZnO thin film as shown in Figure 3 (e). Nevertheless, the high intensity of the optical electric field amplitude occurs mainly in the silicon plate.

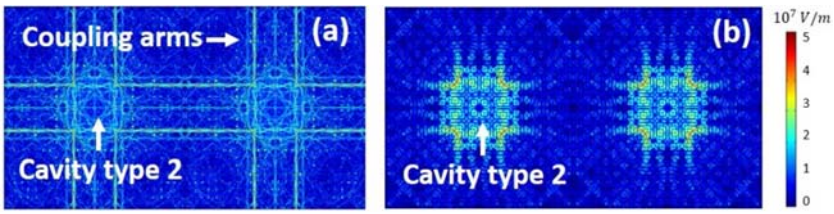

Figure 4. *(a) Two-dimensional top view of the spatial distribution of the optical electric field amplitude established in a type 2 optical cavity that is a part of the square array of micro-cavities in the PhC2, numerically calculated for an incident radiation of 750 nm wavelength showing a coupling effect between the cavities array. (b) A top view of the spatial distribution of the optical electric field amplitude established in the volume determined by a type 2 cavity defined by a ZnO-Si two-layer structure in the PhC2, for an incident light beam with a wavelength of a 1592 nm. Now in (b) the optical electric field is confined practically to the volume determined by the cavity without any coupling established between the cavities.*

On the other hand, the set of cavities defined by a square array of quasi-circular regions (called type 2 resonant cavities), where the circular cylindrical holes have not been milled, constitute by themselves a set of resonant cavities. Figure 4 (a) shows a two-dimensional view (top view) of the optical electric field amplitude established in a representative type 2 optical cavity that is a part of the square array of micro-cavities in PhC2, calculated numerically for an incident radiation with a wavelength of 750 nm. As can be seen in Figure 4 (a), there is a coupling effect between the cavities array. The radiation escapes from one of the cavities shown in Figure 4 (a) into the neighboring cavities given rise to an establishment of a communication loop between them. This contributes to the stimulated emission radiation and thus to the enhancement of optical reflectivity from the PhC2. The coupling effect between the type 2 cavities for a 750 nm wavelength incident light beam on PhC2 can be confirmed in Figure 4 (a) where it is shown how the radiation arms extend from one of the cavities to its nearest neighbors. However, for other light beams with another incident wavelength on the PhC2 a resonant mode could be established in the cavities but they are not necessarily coupled, as shown in Figure 4 (b). Figure 4 (b) shows a top view of the optical electric field established in the volume determined by a type 2 cavity defined by a two-layer structure ZnO-Si (in fact, three layers because a native SiO2 thin film with a thickness of around 5 nm is usually present over the silicon which was taken into account in all calculations) for an incident light beam of 1.592 μm wavelength on the PhC2. Now the optical electric field is confined to the volume determined by the cavity without any coupling established between the cavities. Consequently, as expected, the resonant effects in the cavities studied occur at certain wavelength of radiation and these are determined by the structural parameters, by the spatial distribution between the cavities and by the type of material with which they are built. Therefore, the high reflectance found in the PhC2 studied that contain the array of optical cavities has its origin in the stimulated emission of light occurring mainly in silicon, assisted by the presence of the resonant effects present at specific incident wavelength. In fact, as it was found, these effective resonant modes of the optical electric field can be established in both, the resonant cavities defined by the ZnO:Si mounds over the ZnO-Si substrate, and in the square array of circular micro-cavities configured in the ZnO-Si two-layer substrate.

4. Conclusions

This research has demonstrated the capacity to increase the optical reflectance in two-dimensional photonic structures including an array of optical cavities by means of experimental measurements and exhaustive numerical calculations of their optical properties. From the results obtained, the feasibility of controlling the optical reflectance spectra of a two-dimensional photonic crystal by including an array of optical microcavities was demonstrated. It was obtained that the increase of the optical reflectance amplitude, at certain wavelengths, occurs due to light emissions feasible to stimulate in silicon. The results of numerical calculations of the optical properties of the PhC2 determined that the origin of the increase in the optical reflectance peak it is not the existence of a complete photonic band gap possibly induced by the square array of cavities. Rather, the origin of the high reflectance turns out to be the light emission from the silicon present in the ZnO-Si substrate where the photonic structure was built. Two types of resonant cavities arrays were recognized in the PhC2 sample. Calculations of the optical properties of these two types resonant cavities showed that strong resonant modes of the optical electric field stablished mainly in silicon can favor a stimulated emission of light in the PhC2 which explains its high optical reflectivity. This finding is reasonable since it is more feasible to induce stimulated light emissions in silicon than in ZnO because the former has lower band gap energy than the latter. Nevertheless, it is necessary that effective resonant modes of the optical electric field can be established in both, the resonant cavities defined by a set of ZnO:Si mounds, and in the square array of circular micro cavities configured in the ZnO-Si substrate.

5. Recommendations

1. Conducting the same study varying the structural parameters of photonic crystal such as lattice parameters, air-holes diameter, optical cavities diameter, in order to observe a shift on the peak of optical reflectance.
2. Conducting the same study modifying the square lattice that describes the photonic crystal by a hexagonal lattice and evaluate the effect of this change on the optical reflectance.
3. Study the effect of optical cavities geometry on the optical properties of the photonic structure.

Acknowledgements

The authors would like to thank O. Solís Canto, and W. Antunez Flores, for experimental assistance at Laboratorio Nacional de Nanotecnología, Centro de Investigación en Materiales Avanzados S. C. (CIMAV) México, and V. M. Carrillo for the supply of one of the PhC samples studied.

References

[1] Yablonovitch, E. (1987). Inhibited spontaneous emission in solid-state physics and electronics. Physical Review Letters, 58 (20), 2059.

[2] John, S. (1987). Strong localization of photons in certain disordered dielectric superlattices. Physical Review Letters, 58 (23), 2486.

[3] Notomi M. (2010). Manipulating light with strongly modulated photonic crystals. Reports on Progress in Physics, 73 (9), 096501.

[4] Edagawa K., Kanoko S., & Notomi M. (2008). Photonic Amorphous Diamond Structure with a 3D Photonic Band Gap. Physical Review Letters, 100 (1), 013901.

[5] Pustai D. M., Sharkawy A., Shi S., & Prather D. W. (2002). Tunable photonic crystal microcavities. Applied Optics, 41 (26), 5574.

[6] Chaisakul P., Marris-Morini D., Frigerio J., Chrastina D., Rouifed M.-S., Cecchi S., Crozat P., Isella G., & Vivien L. (2014). Integrated germanium optical interconnects on silicon substrates. Nature Photonics, 8 (6), 482-488.

[7] Smit M., Van der Tol J., & Hill M. (2012). Moore's law in photonics. Laser & Photonics Reviews, 6 (1), 1-13.

[8] Kita S., Nozaki K., & Baba T. (2008). Refractive index sensing utilizing a cw photonic crystal nanolaser and its array configuration. Optic Express, 16 (11), 8174.

[9] Abe H., Narimatsu M., Watanabe T., Furumoto T., Yokouchi Y., Nishijima Y., Kita S., Tomitaka A., Ota S., Takemura Y., & Baba T. (2015). Living-cell imaging using a photonic crystal nanolaser array. Optics Express, 23 (13), 17056.

[10] Krauss T. F., & R. M. De La Rue. (1999). Photonic crystals in the optical regime—past, present and future. Progress in Quantum Electronics, 23 (2), 51-96.

[11] Nellen P. M., Callegari V., & Bronnimann R. (2006). FIB-milling of photonic structures and sputtering simulation. Microelectronic Engineering, 83 (4-9), 1805–1808.

[12] Postigo P. A., Prieto I., Muñoz-Camúñez L. E. & Llorens J. M. (2017). Optical coupling of double L7 photonic crystal microcavities for applications in quantum photonics, 19th International Conference on Transparent Optical Networks (ICTON), pp. 1-5.

[13] Chow E., Lin S. Y., Johnson S. G., & Joannopoulos J. D. (2002). Transmission measurement of quality factor in two-dimensional photonic-crystal microcavity. Proceedings of SPIE, 4646, 199-204.

[14] Sukhoivanov, I. A., & Guryev, I. V. (2009). Photonic Crystals: Physics and Practical Modeling (Berlin Heidelberg: Springer).

[15] Joannopoulus, J. D., Johnson, S. G., Meade, R. D., & Winn, J. N. (2008). Photonic Crystals: Molding the Flow of Light (Princeton NJ USA: Princeton University Press).

[16] Hennessy K., Badolato A., Winger M., Gerace D., Atatüre M., Gulde S., Fält S., Hu E. L., & Imamoğlu A. (2007). Quantum nature of a strongly coupled single quantum dot-cavity system. Nature, 445, 896–899.

[17] Hughes S. (2007). Coupled-Cavity QED Using Planar Photonic Crystals. Physical Review Letters, 98 (8), 083603.

[18] Majumdar A., Rundquist A., Bajcsy M., Dasika V. D., Bank S. R., & Vučković J. (2012). Design and analysis of photonic crystal coupled cavity arrays for quantum simulation. Physical Review B, 86 (19), 195312.

[19] Murillo J. G., Rodríguez-Romero J., Medina-Vázquez J. A., González-Ramírez E. Y., Álvarez-Herrera C., & Gadsden H. (2020). Iridescence and thermal properties of Urosaurus ornatus lizard skin described by a model of coupled photonic structures. Journal of Physics Communications, 4, 015006.

[20] Carrillo-Vázquez V. M., & Murillo J. G. (2015). Effect of patterned coupled optical micro-cavities in twodimensional Si-ZnO hybrid photonic structure. Journal of Physics: Conference Series, 582, 012053.

[21] Snyman LW, Xu K. & Polleux J.-L. (2020). Micron and Nano-Dimensioned Silicon LEDs Emitting at 650 and 750-850 nm Wavelengths in Standard Si Integrated Circuitry. IEEE Journal of Quantum Electronics, 56, 1–10.

[22] Dal Negro L., Cazzanelli M., Pavesi L., Ossicini S., Pacifici D., Franzó G., Pirolo F., & Iacona F. (2003). Dynamics of stimulated emission in silicon nanocrystals, 82 (26), 4636–4638.

[23] Cohen-Tannoudji C., Dupont-Roc J., & Grynberg G. (1992) Atom-Photon Interactions: Basic Processes and Applications (New York: Wiley).

[24] Englund D., Faraon A., Fushman I., Stoltz N., Petroff P., & Vučković J. (2007). Controlling cavity reflectivity with a single quantum dot. Nature, 450, 857-861.

[25] Purcell E. M. (1946) Spontaneous Emission Probabilities at Radio Frequencies. Physical Review Letters, 69, 681.

[26] Gerard J. M., & Gayral B. (1999). Strong Purcell effect for InAs quantum boxes in three-dimensional solid-state microcavities. Journal of Lightwave Technology, 17, 2089–2095.

[27] Sanchis L., Cryan M. J., Pozo J., Craddock I. J., & Rarity J. G. (2007). Ultrahigh Purcell factor in photonic crystal slab microcavities. Physical Review B, 76 (4), 045118.

[28] Akahane Y., Asano T., Song B.-S., & Noda S. (2005). Fine-tuned high-Q photonic-crystal nanocavity. Optics Express, 13, 1202.

[29] Romeira B., & Fiore A. (2018). Purcell effect in the stimulated and spontaneous emission rates of nanoscale semiconductor lasers. EEE Journal of Quantum Electronics, 54, 1–12.